Sensors & Transducers, Vol. 162 , Issue 1, January 2014, pp. 292-298

www.sensorsportal.com

Sensors & Transducers

http://www.sensorsportal.com

A Compliant Control Method Based on Force Sensors on Robot End-effectors for Live-working

[1, 2] Huanbing GAO, [2] Shouyin LU, [2] Tao WANG

[1] School of Control Science and Engineering, Shandong University, Jinan, 250014, China

[2] School of Information and Electrical Engineering, Shandong Jianzhu University, Jinan, 250101, China

[1] Tel.:+8613853144613, fax: +8653186361957

[1] E-mail: gaohuanbing@163.com

Received: 9 October 2013 /Accepted: 9 January 2014 /Published: 31 January 2014

Abstract: This paper proposes a force control method for the live-working robot. Some live-working task requires larger stiffness such as pushing and butting when replacing cross arm or insulator. Two arms are attached on the live-working robot to meet this requirement and other need for cooperation by two arms. The different kinematic structure of this two arms brings many difficulties to get the dynamic model of the total system. This problem is solved by the proposed control scheme, the main idea of which is two arms could be considered as one arm. The force control method for the exact force control is based on the compliant relationship of the dual arms and the environment. The developed control scheme is experimentally tested on the live-working robot, and the experimental investigation concerns it has short computation time and can successfully tracking force. *Copyright © 2014 IFSA Publishing, S. L.*

Keywords: Compliant control, Live-working, Force sensor.

1. Introduction

Live-working is an efficient way to reduce the repair time when there is a power failure and improve the reliability of power supply. The live-working robot, live-working on distribution network under 10 kV instead of the operator, can greatly reduce the labor intensity and risk of working in high-voltage electronic field.

The live-working robot must to do some heavy-load and high-acceleration task such as pressing the fixture of cross arm and insulator. It would greatly increase the mean load of a working cycle and reduce the useful service life of mechanical transmission system, so redundant drive must be adopted. In additionally, many living-working cannot be accomplished by a single robot arm, then two arms are equipped on our live-working robot to work cooperatively and enhance the drive ability. One robot arm is used to do all the live-working tasks, named working robot, while the other arm serves the tasks one arm cannot undertake, called assistive arm. However, the stiffness of the mechanical transmission system is too large to lead to the problem of non-synchronization between the drive unit by the motion error. The consequence of non-synchronization is the surge of the mean load of a working cycle. Force feedback control can resolve this problem, while force sensor with good dynamic characteristics and strong carrying capacity is required.

In consequence, a lot of research has developed compliant control theories for pushing objects with humanoid robots. Ref. [1] extends a full-body balancing controller by simultaneously controlling the reaction forces of both hands using dual-arm force control. Ref. [2] presents force control in single degree of freedom dual arm space robot for cooperative manipulation by two arms. The work uses impedance control to achieve both the objectives, i.e. force control during gripping and trajectory control during docking. In Ref. [3], a general impedance control scheme is adopted, which encompasses a centralized impedance control strategy, aimed at conferring a compliant behavior at the object level, and a decentralized impedance control, enforced at the end-effector level, aimed at avoiding large internal loading of the object. In Ref. [4], a sliding mode controlled dual arm robotic system was designed and PID controller was also applied to it. Ref. [5] proposes a set-point regulation method for a center-of-mass of a dual arm robot composed of a waist and arms. The COM can be controlled by using a COM Jacobian which relates to the joint motion and the COM motion.

Most of the researches are focused on theoretical problem, but there is only a few researcher studied about the application of industrial robot especially live-working robot. So, this research presents how to apply the dual-arm robot to coordinate to accomplish some especial live-working.

2. The Proposed Method

The live-working robot, as shown in Fig. 1, is composed of a mobile truck, an insulated elevating bucket arm, a master control room, a working robot arm, a assistive robot arm, video monitor system and other accessories.

Dual-arm robot can achieve some goals which single-arm robot cannot carry out. Fig. 2 illustrates typical live-working tasks which should be executed by multiple dual-arm robot. Fig. 2(a) shows the closed-chain structure of dual arms to handle the occasions requiring high rigidity such as pushing and butting when replacing cross arm or insulator. Fig. 2(b) shows carrying the bulky or heavy objects, e.g. across arm. Fig. 2(c) is some part mating tasks such as twisting the screw to fix the power line.

Dual-arm robot can be considered as a force redundant System, then the force distribution between the 2 arms is put forward, which can be divided into two categories: load sharing and load balancing. The internal force can balance the system but not influence the motion of the system, which is beneficially utilized to grab, bend, and shear object grasped by the 2 arms.

Master-Slave control structure is widely used in dual-arm system, but it cannot actually achieve load distribution, because measuring force is only by one robot arm while the other one just follows to satisfy the kinematic constraint.

To overcome the shortcoming of the Master-Slave control scheme, symmetric control algorithm has been proposed in which two arms with force/torque sensors at their wrist simultaneously regulate force and position. Symmetric control algorithm can only apply to 2 robot arms with identical kinematic structure, so we should modify the symmetric control algorithm for our asymmetric robot arms [6]. Then we proposed a compliant control algorithm ignoring the kinematic structure with the idea of kinematically considering two arms as one. So the two arms must work on the unified manner rather than cooperative manner. Force error calculated by the data from force/torque sensors installed on each end of the robot arms, is delivered to the minimum actuators coordinates, and then is distributed to the total system actuator coordinates.

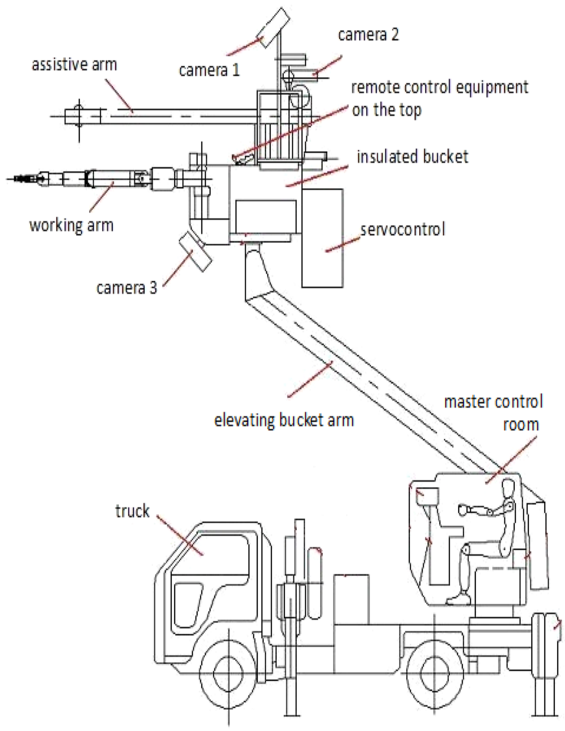

Fig. 1. Mechanical structure of the live-working robot.

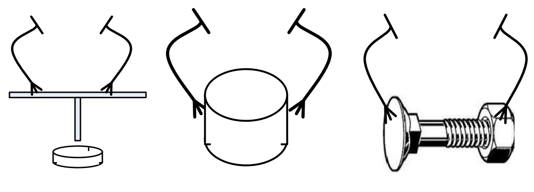

(a) **(b)** **(c)**

Fig. 2. Typical live-working tasks of dual-arm robot.

The position adjustment at the total system actuator coordinates is computed based on the effective stiffness matrix, which is obtained from coordinate transformation between the task coordinates and the total system actuator coordinates. A kinematic modeling for general dual arm systems is to be preceded to support the asymmetric compliant control algorithm.

In order to verify the validity of this method, we discuss a problem of force control for two arms sharing the load shown in Fig. 2(a). A object is hold by two robot arms, push to a stiffness level known environment. In this process, a certain or certain kind of force is required. Calculations and experiments indicate that the force tracking should be completed in 1 second unless it will lead the device damaging or power line shaking. The last test shows that our control strategy can meet the requirement.

3. Research Method

3.1. Structure of the Robot Arms

There are 2 arms on the live-working robot, respectively called working arm and auxiliary arm. The working arm is a hydraulic servo control system with 6 DOF (Degree of Freedom), so it has a compact structure, a lighter weight, and can provide greater power. The maximum carrying capacity of the end-effector is 82 kg and the number became 45 kg when it is fully outstretched. A parallelogram structure is used to distribute the weight of the robot arm to the base via the four connecting rods. The auxiliary arm has a simple structure with 5 DOF for cost saving. The mechanical structure of working arm and assistive arm is shown in Fig. 3.

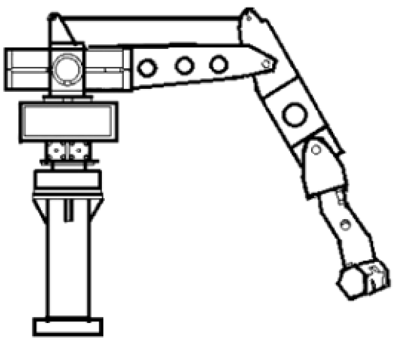

(a) working arm

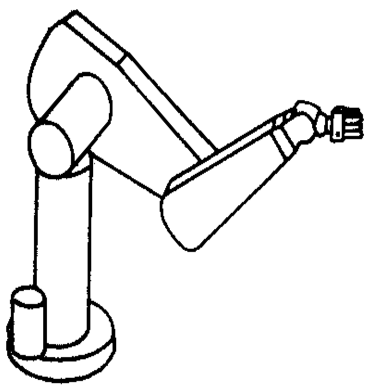

(b) assistive arm

Fig. 3. Mechanical structure of working arm and assistive arm.

Five force sensors are equipped on the 2 arms to measure the force of some different position in the robot. The distribution of force sensors in the robot is shown in Table 1. The column of "Measuring Point" in Table 1 shows which point is measured by this sensor, and "Working Arm – Common Mechanism" means "the contact point of working arm and common mechanism", similarly hereinafter.

There are two levels in the differential motion relationship of the dual-arm working robot. The first level depicts the inner relationship between dependent joint set and independent joint set. The kinematic relationship is obtained by higher-order kinematic constraint equation among the multiple chains. The second layer deals with the relationship between the end-effector motion coordinates and the independent set of actuator coordinates. This mapping is obtained by embedding internal kinematic relationships determined from the first layer into the model of an open-chain kinematic relation.

Table 1. Force sensors distribution.

Sensor ID	Measuring Point	Indicator	Type	Mounting Position
Force Sensor 1	on Target	Force>200N	XH32A-200	End of Standing Part of the Common Mechanism
Force Sensor 2	Working Arm - Common Mechanism	Force>150N	XH32A-150	End of Working Arm
Force Sensor 3	Assistive Arm - Common Mechanism	Force>150N	XH32A-150	End of Assistive Arm
Force Sensor 4	Inner joint of Working Arm	Force>150N	XH32A-150	on Inner Joint of Working Arm
Force Sensor 5	Inner joint of Assistive Arm	Force>150N	XH32B-150	on Inner Joint of Assistive Arm

3.2. Internal Decomposing

Internal kinematics of dual arms id discussed following, which consist of two different serial chains connected to a common hammer moving in a N-dimensional operation space. Because each arm has different number of joint, we should choose a common parameter in a certain coordinate. Some higher-order kinematics such as velocity and acceleration at the end-effector coordinate are same, so we choose end-effector coordinate as an intermediate coordinate to determine the internal kinematic relationship [7].

The generalized velocity of the end-effector (v) can be expressed directly in terms of ${}_r\dot{\varphi}$, the joint velocities of the r^{th} open-chain structure, just shown in Eq. (1).

$$v = [{}_rJ]\,{}_r\dot{\varphi} \qquad r = 1,2 \tag{1}$$

$[{}_rJ]$ is the Jacobian matrix, which defined the relationship between Descartes coordinate vector and the joint coordinate vector. Eq. (1) depicts that there are N related algebraic equations between one joint velocity set and other velocity set, shown in Eq. (2).

$$[{}_1J]\,{}_1\dot{\varphi} = [{}_2J]\,{}_2\dot{\varphi} \tag{2}$$

Furthermore, Eq. (2) can be reorganized as Eq. (3), which separating the coordinate velocity sets of each open-chain into dependent ones and independent ones.

$$[{}_1J_a]\,{}_1\dot{\varphi}_a + [{}_1J_p]\,{}_1\dot{\varphi}_p = [{}_2J_a]\,{}_2\dot{\varphi}_a + [{}_2J_p]\,{}_2\dot{\varphi}_p \tag{3}$$

We rewrite Eq. (3) as the form of Eq. (4).

$$[A]\dot{\varphi}_p = [B]\dot{\varphi}_a \tag{4}$$

In Eq. (3) and Eq. (4),

$$[A] = [[{}_1J_p] \quad -[{}_2J_p]] \tag{5}$$

$$[B] = [-[{}_1J_a] \quad [{}_2J_a]], \tag{6}$$

and $\dot{\varphi}_a$, $\dot{\varphi}_p$ respectively denotes the M dimensional independent joint velocity vector and the（M1+M2-M）dimensional dependent joint velocity vector. [A] is a (M1+M2-M)×(M1+M2-M) dimensional matrix, and [B] is an M×M one.

In our live-working robot, [A] is a nonsingular matrix, so we can get the computing formula for $\dot{\varphi}_p$ as

$$\dot{\varphi}_p = [A]^{-1}[B]\dot{\varphi}_a = [G_p^a]\dot{\varphi}_a, \tag{7}$$

where $[G_p^a]$ is just the Jacobian matrix of the dual-arm system. The relationship between the independent joint set and the whole joint set is expressed as Eq. (8) with φ standing for the whole joint set of the system.

$$\dot{\varphi} = [G_a^{\varphi}]\dot{\varphi}_a \tag{8}$$

$[G_a^{\varphi}]$ is a (（M1+M2）×M) matrix which can obtained by Eq. (9).

$$[G_a^{\varphi}] = \begin{bmatrix} [I] \\ [G_a^p]^T \end{bmatrix} \tag{9}$$

3.3. Differential Motion Relationship of Whole System

Since the matrix describing the relationship between the internal constraints and end-parameters has been got, the relationship between the independent joint set and the whole joint set expressed as Eq. (8) can be transform into a open chain model to obtain the relationship between the minimum motion parameters ($\dot{\varphi}_a$) and the operational velocity parameters (v). The rth chain consists of some independent joints and dependent joints, then ${}_r\dot{\varphi}$ can be given by Eq. (10).

$${}_r\dot{\varphi} = \begin{bmatrix} {}_r\dot{\varphi}_a \\ {}_r\dot{\varphi}_p \end{bmatrix} = \begin{bmatrix} {}_rG_a^{\varphi} \end{bmatrix} {}_r\dot{\varphi}_a \tag{10}$$

$\begin{bmatrix} {}_rG_a^{\varphi} \end{bmatrix}$ can be obtained by Eq. (7), and the differential motion equation can be calculated by Eq. (1) substituting Jacobian matrix into, shown as

$$v = [{}_rJ]\,{}_r\dot{\varphi} = [\ G_a^u]\dot{\varphi}_a \ r = 1,2, \tag{11}$$

where

$$[G_a^u] = [{}_rJ][{}_rG_a^{\varphi}] \tag{12}$$

The effective inertial load of the system (T_a^*) referenced to a set of independent joints is expressed by the system's effort sources (T_a and T_p), externally applied loads T_u^L, and effective gravity loads (T_{φ}^G) as follows:

$$T_a^* = [G_a^{\varphi}]^T T_{\varphi} - [G_a^u]^T T_u^L + [G_a^{\varphi}]^T T_{\varphi}^G, \tag{13}$$

where

$$T_{\varphi}^G = \left[[{}_1T_{\varphi}^G]^T [{}_2T_{\varphi}^G]^T \right]^T \tag{14}$$

$${}_rT_{\varphi}^G = \sum_{i=1}^{M_r} [{}_r^iG_{\varphi}^c]^T \, {}_r^iF_G \quad r = 1,2 \tag{15}$$

The gravity loads and inertial load referenced to the independent input set can be calculated from the open-chain dynamics via a virtual work-based transfer method according to $[G_a^{\varphi}]^T$. T_{φ} is the total efforts include the independent T_a and dependent joints T_p, and ${}_r^iF_G$ is the gravity load of the i[th] link of the r*th* chain. ${}_rT_{\varphi}^*$ and ${}_rT_{\varphi}^G$ are the total inertia loads and gravity loads respectively. $[{}^{i}_{r}G^{c}_{\varphi}]$ is the Jacobian matrix denoting the relation between the mass center of the i*th* link of the r*th* chain and the inputs of the r*th* chain [6].

According to the principle of virtual work, the sufficient and necessary condition of equilibrium is that the sum of virtual work by the force of the mass working on any virtual displacement is zero. Assuming that the system is in a state of equilibrium, we can get

$$T_a^* = [G_a^\varphi]^T T_\varphi - [G_a^u]^T T_u^L + [G_a^\varphi]^T T_\varphi^G = 0 \quad (16)$$

Furthermore, considering the number of the active actuators is the minimum value, the relationship between the executing joints and external force can be shown as

$$T_a = [G_a^u]^T T_u^L - [G_a^\varphi]^T T_\varphi^G \quad (17)$$

The linear form of Eq.(20) is

$$\begin{aligned} \delta T_a &= [G_a^u]^T \delta(T_u^L) + \left[\frac{\partial [G_a^u]^T}{\partial \varphi_a}\delta\varphi_a\right] T_u^L \\ &- [G_a^\varphi]^T \delta(T_\varphi^G) - \left[\frac{\partial [G_a^\varphi]^T}{\partial \varphi_a}\delta\varphi_a\right] T_\varphi^G \end{aligned} \quad (18)$$

An external disturbance working on the system, it can be modeled as a spring action system considering independent inputs. So, taking the derivative with respect to φ_a of both sides of Eq.(18), the stiffness equation of the dual arm system can be get as follows

$$\begin{aligned} [K_{aa}] &= -\frac{\partial T_a}{\partial \varphi_a} = [G_a^u]^T [K_{uu}][G_a^u] - \frac{\partial [G_a^u]^T}{\partial \varphi_a} T_u \\ &- [G_a^\varphi]^T [V][G_a^\varphi] + \frac{\partial [G_a^\varphi]^T}{\partial \varphi_a} T_\varphi^G \end{aligned} \quad (19)$$

where

$$[K_{uu}] = -\frac{\partial T_u^L}{\partial u}, \quad (20)$$

$$[V] = -\frac{\partial T_\varphi^G}{\partial \varphi}. \quad (21)$$

The second item, third item and fourth item of Eq. (18) is the additional stiffness effects of the external applied load and gravity load. From another perspective, the compliant matrix of the system reference to the minimum inputs can be represented as

$$[C_{aa}] = [K_{aa}]^{-1}. \quad (22)$$

The effective effort at the minimum actuator site in the case of full actuation is shown as

$$T_a = [G_a^\varphi]^T T_\varphi. \quad (23)$$

Assuming a infinitesimal displacement and a infinitesimal effort, we can get Eq. (24) and Eq. (25) based on Eq. (8) and Eq. (23).

$$\delta\varphi = [G_a^\varphi]\delta\varphi_a \quad (24)$$

$$\partial T_a = [G_a^\varphi]^T \partial T_\varphi \quad (25)$$

$\delta\varphi$ and $\delta\varphi_a$ in Eq.(24) can be given by

$$\delta\varphi = -\left[C_{\varphi\varphi}\right]\delta T_\varphi, \quad (26)$$

$$\delta\varphi_a = -\left[C_{aa}\right]\delta T_a. \quad (27)$$

Thus, the compliant relationship between the total actuator and the minimum actuator, calculated by the range of equations from Eq. (24) to Eq. (27), can be obtained as

$$\left[C_{\varphi\varphi}\right] = [G_a^\varphi][C_{aa}][G_a^\varphi]^T \quad (28)$$

In practice, considering the working condition of the live-working robot, compared to the additional stiffness due to the external effort and gravity loads and joints loads, the stiffness of the environment is usually very large, so Eq. (28) can be simplified as

$$\left[C_{\varphi\varphi}\right] = [G_a^\varphi][G_a^u]^{-1}\left[K_{uu}\right]^{-1}[G_a^u]^{-T}[G_a^\varphi]^T \quad (29)$$

4. Results and Discussion

The block diagram of the proposed compliant control algorithm is shown as Fig. 4. Initially, for the compensated force error δF, the effort δT_a on the minimum inputs is expressed as

$$\delta T_a = [G_a^u]^T \delta F \quad (30)$$

And the effort on the total inputs δT_φ is calculated from the formula relating the minimum inputs to the total inputs, shown as

$$\delta T_\varphi = \left([G_a^\varphi]^T\right)^+ \delta T_a + \left([I] - \left([G_a^\varphi]^T\right)^+ [G_a^\varphi]^T\right)\varepsilon \quad (31)$$

In Eq. (31), the first item is a minimum norm solution and the second item represents an internal load. $\left([G_a^\varphi]^T\right)^+$ is the generalized inverse matrix since $[G_a^\varphi]^T$ is not always a singular matrix. If only a certain number of actuators are activated, $[G_a^\varphi]^T$ could be rebuilt by selecting the corresponding column vectors.

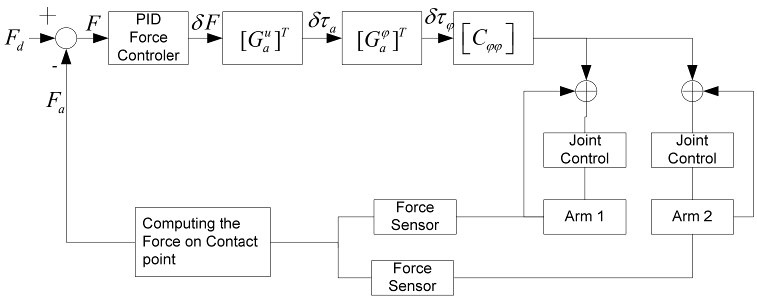

Fig. 4. Block diagram of control algorithm.

Then, according the compliant relationship by Eq. (29), the force error can be eliminated by controlling the rotation angles of each joint. PID force controller can employ to compensate the force and reach good performance on force control [8, 9].

Because the high gear ratio of the manipulator on live-working robot, manipulator dynamics can be neglected. Thus, only the filter dynamics is considered. The interaction force and moment between the dual arms and the environment can be measured by the sensors equipped on each arms and the mass of the knocking tools grasped by two arms is ignored here.

Using the algorithms presented above, experiments were conducted to verify the system's ability to properly control force during a live-working procedure.

The voltages changes of the contacted sensor cells installed on the end of 2 arms and the contact point are recorded through the MATLAB OPC sever, which are then transformed to the sensor pressures and contact forces. Fig. 5 shows the interaction force of the 3 points.

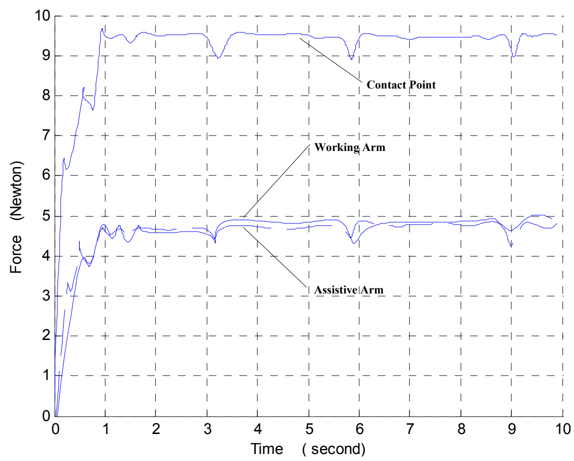

Fig. 5. Interaction force of the 3 points.

Form the figure, it is seen that the algorithm properly controlled the force within 1 second. "1 second" is the safe time limit got by preliminary trials, that is, the device could probably be damaged if the tracking time is longer than 1 second. To compare the performance between our proposed approach and master-slave structure, we also took our robot employ in master-slave control method, but the force tracking time was always between 3 to 5 seconds.

5. Conclusion

A compliant control method and the compliant relationship were proposed for the exact force control of dual arms with different kinematic structure attached on the live-working robot. Main idea of the proposed approach was that two arms could be considered as one arm and the foundation is the data from the force sensors. The approach was tested in the practice live-working of pushing and butting when replacing cross arm or insulator. Actually, this method can be used another force control task in the case of that two robot arms have respective kinematic structure.

Acknowledgments

This work was supported by National High-tech Research and Development Projects (863), under the Grants 2012AA041506.

References

[1]. Shunichi Nozawa, Yohei Kakiuchi, Kei Okada and Masayuki Inaba, Controlling the planar motion of a heavy object by pushing with a humanoid robot using dual-arm force control, in *Proceedings of the IEEE International Conference on Robotics and Automation*, May 14-18, 2012, pp. 1428-1435.

[2]. Haresh Patolia, P. M. Pathak, S. C. Jain, Force control in single DOF dual arm cooperative space robot, in *Proceedings of Spring Simulation Multiconference*, April 11, 2010, pp. 1-8.

[3]. Fabrizio Caccavale, Pasquale Chiacchio, Alessandro Marino, and Luigi Villani, Six-DOF impedance control of dual-arm cooperative manipulators, *IEEE/ASME Transactions on Mechatronics*, Vol. 13, No. 5, 2008, pp. 576-586.

[4]. Nurkan Yagiz, Yuksel Hacioglu and Yunus Ziya Arslan, Load transportation by dual arm robot using sliding mode control, *Industrial Robot*, Vol. 38, No. 2, 2011, pp. 172-185.

[5]. Kwanghyun Ryu, Yonghwan Oh, Minjoon Choi, COM control of dual arm robot using COM Jacobian, in *Proceedings of the IEEE International Conference on Automation Science and Engineering*, 2012, pp. 1071-1073.

[6]. H. J. Yeo, S. J. Lee, I. H. Suh, B. J. Yi, S.-R. Oh, External force control using cooperating two arms with general kinematic structures, in *Proceedings of the IEEE International Workshop on Robot and Human Communication*, November 11, 1996, pp. 388-394.

[7]. S. Arimoto, H. Hashiguchi, M. Sekimoto, and R. Ozawa, Generation of natural motions for redundant multi-joint systems: A differential geometric approach based upon the principle of least actions, *Journal of Robotic Systems*, Vol. 22, No. 11, 2005, pp. 583-605.

[8]. P. Rocco, Stability of PID control for industrial robot arms, *IEEE Transactions on Robotics and Automation,* Vol. 12, No. 4, 1996, pp. 606–614.

[9]. W. Gueaieb, F. Karray, and S. Al-Sharhan, A robust hybrid intelligent position/force control scheme for cooperative manipulators, *IEEE/ASME Transactions on Mechatronics,* Vol. 12, No. 2, 2007, pp. 109–125.